

Anderson localization of partially-incoherent light

D. Čapeta,¹ J. Radić,¹ A. Szameit,² M. Segev,² and H. Buljan¹

¹*Department of Physics, University of Zagreb, PP 332, 10000 Zagreb, Croatia*

²*Technion, Israel Institute of Technology, Haifa, Israel*

(Dated: July 11, 2018)

We study Anderson localization and propagation of partially-spatially incoherent wavepackets in linear disordered potentials, motivated by the insight that interference phenomena resulting from multiple scattering are affected by the coherence of the waves. We find that localization is delayed by incoherence: the more incoherent the waves are, the longer they diffusively spread while propagating in the medium. However, if all the eigenmodes of the system are exponentially localized (as in one- and two-dimensional disordered systems), any partially-incoherent wavepacket eventually exhibits localization with exponentially-decaying tails, after sufficiently long propagation distances. Interestingly, we find that the asymptotic behavior of the incoherent beam is similar to that of a single instantaneous coherent realization of the beam.

PACS numbers: 42.25.Dd, 42.25.Kb, 72.15.Rn

The phenomenon of Anderson localization was conceived in the context of disordered electronic systems [1], however, localization phenomena have been extensively studied also in other systems [2–17] including optics [2, 3, 5–14] and ultracold quantum gases [15–17]. For a direct observation of the phenomena, optical and ultracold atomic systems have some profound advantages over the condensed matter systems: the influence of the environment such as thermal fluctuations and phonons can be minimized to become negligible, and nonlinearity/interactions can be controlled and virtually turned off. Nonlinearity in optics can be controlled by the intensity of light, whereas interactions of ultracold gases can be tuned via Feshbach resonances. In contrast, electron-electron and electron-phonon interactions are always present in condensed matter systems. These influences are important since they affect interference, and Anderson localization arises from interference among multiple scattering events from disorder in the medium.

Here we address Anderson localization of waves with imperfect coherence. We investigate whether an initial finite-size partially-incoherent wavepacket would spread through a linear disordered potential, or would its spreading be stopped by virtue of disorder? We demonstrate our findings on an optical (1+1)D potential, and discuss the implications of our results to other wave systems in nature. A superficial answer to the question above may be that, since incoherence destroys interference effects, a sufficiently incoherent wavepacket will diffuse through the random medium without ever being localized. However, from the theory of coherence [18] it is known that an incoherent wave can be thought of as a superposition of coherent modes with stochastically varying coefficients. Each of these coherent modes is expected to undergo localization, hence the entire wavepacket should localize. Our study reveals that coherence indeed affects the properties of evolving wavepackets, in a sense that more incoherent beams spread more while propagating through the random medium. However, if the system's eigenmodes are all localized, as is the case for all one-dimensional

[(1+1)D] and two-dimensional [(2+1)D] fully disordered systems [19], the incoherent wavepacket will eventually become Anderson localized. Finally, we find that a typical instantaneous coherent speckled realization of the incoherent beam exhibits the same asymptotic behavior as the time-averaged incoherent wavepacket.

The idea that localization could be observed in optics dates back to the beginning of the 80s [2, 3]. The experiments on so-called weak localization [4], which can be pictured in terms of a coherent backscattering process, were soon to follow [5, 6]. Experiments on strong localization in random media were performed in various systems [8–10]. In 1989, a non-traditional idea for observing localization was proposed: the transverse localization scheme [7], which exploits the equivalence between the Schrödinger equation and the paraxial wave equation for light. Indeed, this scheme was used for a clear demonstration of Anderson localization in random optical lattices [11], for the observation of Anderson modes [12], and localization near an interface [13]. All of these have dealt with fully coherent waves only. In a different domain, the propagation of partially-incoherent light in random media is a subject of considerable interest (e.g., see [20]). However, in the context of localization, the only studies on incoherent light were on enhanced backscattering [21, 22], which is considered a precursor to Anderson localization. To the best of our knowledge, strong localization with partially-incoherent waves has never been studied.

Consider the propagation of a partially-spatially incoherent optical beam, linearly polarized, originating from a quasimonochromatic continuous-wave source. Such a beam can be constructed by sending a laser beam through a rotating diffuser (e.g., see [23]). Its state at a given propagation distance z can be described in terms of the mutual coherence function [18],

$$B(x_1, x_2, z) = \langle E^*(x_2, z, t)E(x_1, z, t) \rangle_t, \quad (1)$$

where $\langle \dots \rangle_t$ is the time-average, and E is the stochastic field. Instead of $B(x_1, x_2, z)$, the state of the system can be described by an orthonormal set of modes $\psi_j(x, z)$

($j = 1, 2, \dots$), and their modal weights λ_j , which are obtained from the eigenvalue equation [18]

$$\int dx_2 B(x_1, x_2, z) \psi_j(x_2, z) = \lambda_j \psi_j(x_1, z), \quad (2)$$

i.e., $B(x_1, x_2, z) = \sum_j \lambda_j \psi_j^*(x_2, z) \psi_j(x_1, z)$.

We analyze linear propagation of such a beam in the transverse localization scheme [7], in a waveguide array defined by $n^2 = n_0^2 + 2n_0\delta n(x)$, where n_0 is a constant term, while $\delta n(x)$ describes disorder. The propagation of the beam along the z axis is governed by the Schrödinger equation [11]

$$i \frac{\partial \psi}{\partial z} = -\frac{1}{2k} \frac{\partial^2 \psi}{\partial x^2} - \frac{\delta n(x)k}{n_0} \psi, \quad (3)$$

where $k = n_0\omega/c$ is the wave vector, ω is the temporal frequency of the beam carrier, and c is the speed of light.

In our simulations, we analyze the evolution of Gaussian input beams:

$$B(x_1, x_2, z = 0) = I_0 \exp\left[-\left(\frac{x_1 + x_2}{2\sigma_I}\right)^2 - \left(\frac{x_1 - x_2}{\sigma_C}\right)^2\right], \quad (4)$$

where σ_I and σ_C are the spatial and the coherence widths of the beam, respectively. In disordered media, the propagation depends on the particular realization of the random potential $\delta n(x)$. Thus, to obtain meaningful results, one needs to observe the evolution of the mutual coherence for many realizations of the disorder, and calculate the disorder ensemble average [11]: $\langle B(x_1, x_2, z) \rangle_d$.

The disordered potential used in our simulations is illustrated in Fig. 1(a). The index of refraction varies randomly (with uniform distribution) between $\delta n = 0$ and $\delta n = 1.2 \times 10^{-3}$. The width of every rectangular potential unit shown in Fig. 1(a) is $2.7 \mu\text{m}$, but their mutual distances are random: first we fix the leftmost rectangle in its position, and then add the adjacent ones to the right such that their distance (center to center) is between 5 and $9 \mu\text{m}$ (chosen at random), and so on. Such a disordered medium can be created experimentally by using the ultrafast direct laser writing technique [13].

Because the system is linear, the evolution of the beam (in a given realization of the disorder) can be described in terms of the modes of the system u_n and their propagation constants β_n , which obey

$$\beta_n u_n = \frac{1}{2k} u_n''(x) + \frac{\delta n(x)k}{n_0} u_n. \quad (5)$$

Every initial coherent wave $\psi_j(x, 0)$ is projected onto the system's modes u_n : $c_{j,n} = \int dx \psi_j(x, 0) u_n^*(x)$, yielding $\psi_j(x, z) = \sum_n c_{j,n} u_n(x) e^{i\beta_n z}$, that is,

$$B(x_1, x_2, z) = \sum_{j,n,m} \lambda_j c_{j,n}^* c_{j,m} u_n^*(x_2) u_m(x_1) e^{i(\beta_m - \beta_n)z}. \quad (6)$$

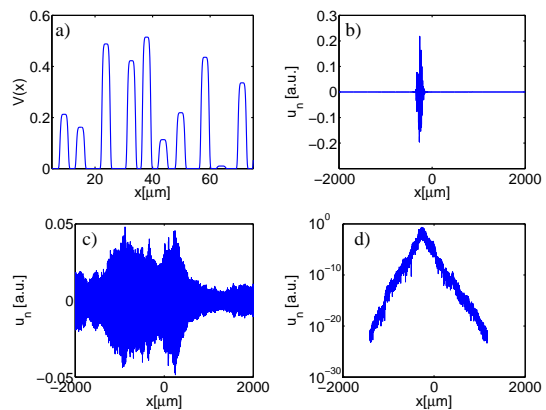


FIG. 1: The disordered potential and its eigenmodes. (a) Small section of the dimensionless disordered potential $V(x) = -2\delta n(x)(kx_0)^2/n_0$, where $k = 2\pi n_0/\lambda$, $\lambda = 514 \text{ nm}$, $x_0 = 1 \mu\text{m}$, $n_0 = 1.45$. (b,c) Typical eigenfunctions (Anderson states) of the structure with a smaller (b) and larger (c) spatial extent, in a sample of width $L = 4 \text{ mm}$. (d) Logarithmic plot of $|u_n(x)|$ from (b) with exponentially decaying tails, which are the fingerprint of Anderson localization.

It is reasonable to conjecture that after sufficiently long propagation z , the beam will dephase and attain the following form of the mutual coherence:

$$B(x_1, x_2, z \rightarrow \infty) = \sum_{j,n} \lambda_j |c_{j,n}|^2 u_n^*(x_2) u_n(x_1). \quad (7)$$

From Eqs. (6) and (7) we clearly see that, if the medium is infinitely broad, and if the potential is fully random, then, since all the eigenmodes u_n are Anderson localized, any initial finite-width partially-incoherent beam will not diffuse during propagation despite its incoherence. One can expect that, after sufficiently long propagation, the tails of the incoherent beam will become exponentially decaying: $B(x, x, z \rightarrow \infty) \propto \exp(-\gamma|x|)$, with γ corresponding to the excited eigenmode u_n which has the slowest decay. However, in reality, all samples have finite transverse (L) and longitudinal (Z) size; hence, we explore the finite-size effects.

First we calculate the eigenvectors/eigenvalues of the potential $\delta n(x)$. We use the LAPACK implementation of the MRRR algorithm [24], with Dirichlet boundary conditions $u_n = 0$ at the boundaries of the medium ($x = \pm L/2$). Typical eigenfunctions are shown in Figs. 1(b)-(d). Up to some critical value of n , the spatial extent of the eigenfunctions u_n is smaller than L [see Fig. 1(b)], whereas above this value they extend to one or both of the boundaries [see Fig. 1(c)]. The localized eigenfunctions are a consequence of Anderson localization, which can be seen from Fig. 1(d), where we depict $|u_n(x)|$ on a logarithmic scale. Clearly, the amplitude of $u_n(x)$ decays exponentially, $\log |u_n(x)| \propto \exp(\gamma_n x)$, which is a fingerprint of Anderson localization in this (1+1)D system. From these eigenmodes, we calculate their Lyapunov exponents as follows: We form a set $\{|u_n(x_{\max})|\}$ of local

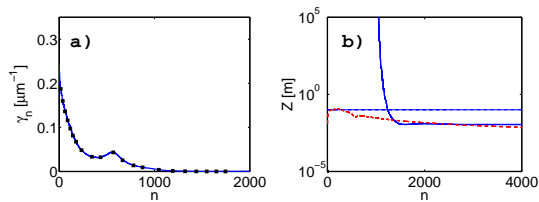


FIG. 2: (a) Lyapunov exponents γ_n extracted from the eigenfunctions u_n (solid blue line) and via the transfer matrix approach (black squares). Shown are averages over 40 different realizations of the random potential; the standard deviation is smaller than the thickness of the line. (b) The Thouless (solid blue line) and the Heisenberg (dashed red line) times (propagation distances) vs. n for the system with $L = 4$ mm. Horizontal line depicts $Z = 10$ cm. See text for details.

maxima of $|u_n(x)|$, and then fit $-\gamma_n|x-x_c|+b$ to the set of points $\log|u_n(x_{\max})|$, to obtain γ_n for every u_n . For the lowest eigenstates, which have too few local extrema, $|u_n|$ was fitted. The Lyapunov exponents, averaged over 40 different realizations of the random potential, are shown in Fig. 2(a) as a function of n ; the standard deviation is as small as the thickness of the line implying that the Lyapunov exponents have the self-averaging property. In order to underpin our results, we have also calculated the Lyapunov exponents via the transfer matrix approach [19], i.e., for an essentially infinite sample, and obtained nondistinguishable results [black squares in Fig. 2(a)]. Evidently, the overall trend is such that the Lyapunov exponents decrease with increasing n (decreasing β_n), except for a small hump, which is a consequence of relatively small fluctuations in distances between adjacent potential peaks [Fig. 1(a)] (if we allow larger fluctuations the hump disappears).

In a realistic experimental situation with finite-size samples, a partially-incoherent initial wavepacket is likely to excite both types of modes: modes that are Anderson localized on a scale smaller than L , and modes extending to the boundary. In order to investigate the finite-size effects, we first evolve (numerically) an initial wavepacket with absorbing boundary conditions [Figure 3 (a)], and then repeat the simulation with reflecting boundary conditions [Figure 3 (b)] (both can be realized in experiments). The initial size of the beam is $\sigma_I = 10 \mu\text{m}$, and the degree of coherence varies: $\sigma_C = 1, 3$, and $5 \mu\text{m}$; $L = 4$ mm. In our simulations, absorbing boundary conditions are included as an imaginary index of refraction, $\Im\delta n_{\text{abs}} > 0$, which is present *only* close to the sample edges: $\delta n_{\text{abs}} = 0$ for $|x| < 0.96 \frac{L}{2}$.

From the simulations with absorbing edges we find that, after sufficiently long propagation, the intensity structure has exponentially decaying tails: $\langle I \rangle_d \propto \exp(-\gamma|x|)$. All graphs have approximately the same value for the slope, $\gamma = 3.2 \times 10^{-3} \mu\text{m}^{-1}$. This is in accordance with our analysis of eigenstates. Namely, the part of the beam exciting eigenstates which touch (or are in the very vicinity of) the edges, gets absorbed during

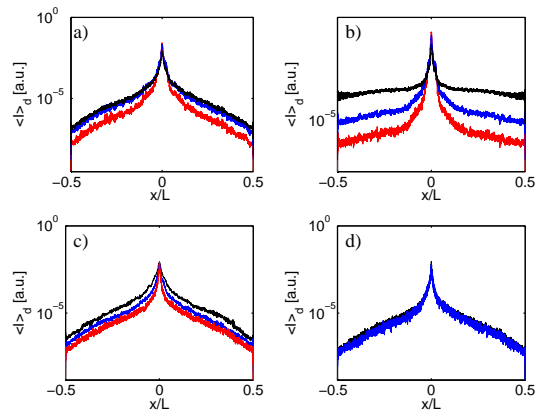


FIG. 3: Intensities of the incoherent beam after $Z = 10$ cm of propagation, for different system parameters, averaged over 40 realizations of the disorder. (a,b) Beam intensity for absorbing (a) and reflecting (b) boundary conditions for beams with $\sigma_I = 10 \mu\text{m}$, and $\sigma_C = 1 \mu\text{m}$ (top black line), $3 \mu\text{m}$ (middle blue line), and $5 \mu\text{m}$ (bottom red line); $L = 4$ mm. (c) Beam intensity for absorbing boundary conditions and three values of L : 2, 4, and 8 mm (top to bottom) [$\sigma_I = 10 \mu\text{m}$, $\sigma_C = 1 \mu\text{m}$]. (d) The intensity for one specific instantaneous initial realization of the incoherent field (lower blue line), and the time-averaged intensity (upper black line) [$\sigma_I = 10 \mu\text{m}$, $\sigma_C = 1 \mu\text{m}$, $L = 8$ mm, absorbing boundary conditions].

propagation. The remaining part of the beam excites only exponentially decaying eigenstates, which yields the intensity plotted in Fig. 3(a). The value of γ found from graphs in Fig. 3(a) correspond to the slowest decay rate γ_n of the eigenstate u_n which is excited, and which does not overlap with the absorbing boundary, i.e., $\langle u_n | \delta n_{\text{abs}}(x) | u_n \rangle \approx 0$ (one should take into account factor 2 because $I = \langle |E|^2 \rangle_t$).

At this point it is worthy to consider the Thouless (Z_T) and Heisenberg (Z_H) times (propagation distances) in our system. The former tells us the average time it takes for a particle (with some energy) to diffuse across the sample, and the latter is the longest time the particle can travel inside the sample without visiting the same region twice (e.g., see [14] and Refs. therein). In our case Z_T corresponds to the inverse linewidth ($1/\Delta\beta_n$) of the eigenstates with absorbing boundary conditions. In calculating $Z_T(n)$ we have averaged $1/\Delta\beta_n$ over 20 adjacent eigenstates, and then over 40 realizations of the potential. In the same fashion we have calculated the average inverse level spacing which yields the Heisenberg time $Z_H(n)$. Figure 2(b) shows Z_T and Z_H vs. n . Evidently the Thouless time is effectively infinite for $n < 1200$ indicating Anderson localization in our finite sample, whereas for greater n values the two times are on comparable scales. From Fig. 3(a), we conclude that the more coherent the light is - the stronger the localization effect is, in a sense that less power is absorbed by the walls. For the samples used in our simulations the rate of decaying tails are identical for all values of σ_C , because in every case the highest of the localized modes

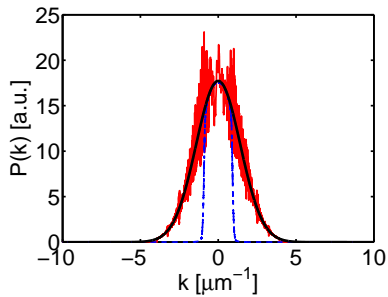


FIG. 4: Spatial power spectrum of the incoherent beam after $Z = 10$ cm of propagation in a disordered medium with absorbing (thin dashed blue line) and reflecting (solid red line) edges, for an initial beam (thick solid black line) defined by $\sigma_I = 10 \mu\text{m}$, $\sigma_C = 1 \mu\text{m}$. All plots are averages over 40 realizations of the disorder.

was excited.

It is interesting to note that the values γ obtained after transport simulations (expansion) *depend* on the size of the sample L , and scale approximately as $\gamma \propto L^{-1}$. We checked this trend for $L = 2, 4$, and 8 mm, see Fig. 3(c). The observed scaling is found to be in agreement with the studies conducted in [25], where it was shown that the logarithm of the dimensionless resistance scales as the length in case of localization.

Figure 4 shows a typical change in the spatial power spectrum (closely related to the spatial coherence) for propagation dynamics with different boundary conditions. In the case of absorbing edges, there is a clear cut off in k -space above which the modes are no longer localized on a scale smaller than L . The modes u_n comprised of plane waves (via Fourier transform) with k values above the cut-off evidently spread to the absorbing boundaries of the medium. This process also increases the overall coherence of the beam, because it has fewer and fewer modes as it propagates. In contrast, for reflecting boundary conditions, the final power spectrum has the same overall shape as the initial spectrum, with fluctuations on top of the average shape.

A partially-spatially incoherent (quasimonochromatic) beam can be thought of as a train of fully coherent fields with intricate field structures, which are replaced on a time scale $\sim \Delta t_c$ (the temporal coherence time); quasimonochromatic means that $\Delta t_c \gg Z/c$. In experiments, one instantaneous realization of the incoherent field can be observed by simply stopping the rotation of the dif-

fuser [23]. Interestingly, we find that one instantaneous field realization will asymptotically have exponentially-decaying tails similar to those of the time-averaged intensity, as illustrated in Figure 3(d) (both graphs are averaged over disorder). Thus, the localization of a partially-incoherent field can be thought of as the localization of many instantaneous coherent speckled structures, whose ensemble average produces localized mutual coherence. The exponential decay of the asymptotic intensity evidently depends both on the degree of coherence and the spatial structure of the input field.

We can extend our conclusions to hold for spatially and temporally incoherent beams of light ($\Delta t_c < Z/c$), such as the one constructed from an incandescent light bulb in Ref. [26]. In this case, a space-time mutual coherence function describing the beam can be transformed into the space-frequency domain [18, 27]. Because our results hold for every frequency component separately (with somewhat different numerical values because different frequencies experience different diffraction), due to linear superposition, it is evident that they also hold for the whole spatially and temporally incoherent beam.

Before closing, we note that our results correspond to partially condensed *noninteracting* Bose-Einstein condensates (BECs) in 1D disordered potentials. As an interesting consequence of dimensionality, we note that our results also pertain to the strongly interacting 1D Bose gases [28], and noninteracting 1D Fermi gases, which are modeled by identical equations [29]. To mimic partially-condensed interacting BECs [30], one should include nonlinearity, which we leave for further studies.

In conclusion, we have predicted the properties of Anderson localization of partially spatially-incoherent beams in disordered linear (1+1)D photonic structures. We conclude that more incoherent light will diffusively spread more through the random medium than coherent light, however, the incoherent wavepacket will display exponentially decaying tails after sufficiently long propagation. We have discussed the finite size effects, and extended our conclusions for spatially and temporally incoherent light beams.

This work was supported the Croatian-Israeli scientific cooperation program funded by the Ministries of Science of the State of Israel and the Republic of Croatia. AS thanks the Leopoldina - The German Academy of Science (grant LPDS 2009-13), and HB the MZOS grant 119-0000000-1015.

[1] P.W. Anderson, Phys. Rev. **109**, 1492 (1958).
[2] S. John, Phys. Rev. Lett. **53**, 2169 (1984).
[3] P.W. Anderson, Phil. Mag. B **52**, 505 (1985).
[4] E. Akkermans, R. Maynard, J. Phys. Lett. **46**, 1045 (1985).
[5] M.P. Van Albada, A. Lagendijk, Phys. Rev. Lett. **55**,

2692 (1985).
[6] P-E. Wolf, and G. Maret, Phys. Rev. Lett. **55**, 2696 (1985).
[7] H. De Raedt, A. Lagendijk, P. de Vries, Phys. Rev. Lett. **62**, 47 (1989).
[8] D.S. Wiersma, P. Bartolini, A. Lagendijk, R. Righini,

- Nature **390**, 671 (1997).
- [9] A.A. Chabanov, M. Stoytchev, A.Z. Genack, Nature **404**, 850 (2000).
- [10] M. Störzer, P. Gross, C.M. Aegerter, G. Maret, Phys. Rev. Lett. **96**, 063904 (2006).
- [11] T. Schwartz, G. Bartal, S. Fishman, and M. Segev, Nature **446**, 52 (2007).
- [12] Y. Lahini *et al.*, Phys. Rev. Lett. **100**, 013906 (2008).
- [13] A. Szameit *et al.*, Opt. Lett. **35**, 1172 (2010).
- [14] A. Lagendijk, B. van Tiggelen, and D.S. Wiersma, Physics Today, August 2009, page 24.
- [15] J. Billy *et al.*, Nature **453**, 891 (2008).
- [16] G. Roati *et al.*, Nature **453**, 895 (2008).
- [17] For a recent review see L. Sanchez-Palencia and M. Lewenstein, Nature Phys. **6**, 87 (2010).
- [18] L. Mandel and E. Wolf, *Optical Coherence and Quantum Optics* (Cambridge Press, New York, 1995).
- [19] E.N. Economou, *Green's Functions in Quantum Physics* (Springer, Berlin, 2006).
- [20] G. Gbur and E. Wolf, J. Opt. Soc. Am. A **19**, 1592 (2002).
- [21] A. Wax, S. Bali, and J. E. Thomas Phys. Rev. Lett. **85**, 66 (2000).
- [22] Y.L. Kim *et al.*, Opt. Lett. **29**, 1906 (2004).
- [23] M. Mitchell, Z. Chen, M. Shih, and M. Segev, Phys. Rev. Lett. **77**, 490 (1996).
- [24] Inderjit S. Dhillon, PhD thesis, EECS Department, University of California, Berkeley (1997).
- [25] P.W. Anderson, D.J. Thouless, E. Abrahams, and D.S. Fisher, Phys. Rev. B **22**, 3519 (1980).
- [26] M. Mitchell and M. Segev, Nature (London) **387**, 880 (1997).
- [27] H. Buljan, A. Šiber, M. Soljačić, and M. Segev, Phys. Rev. E **66**, 035601 (2002).
- [28] J. Radić *et al.*, Phys. Rev. A **81**, 063639 (2010).
- [29] H. Buljan *et al.*, Phys. Rev. A **74**, 043610 (2006).
- [30] H. Buljan, M. Segev, and A. Vardi, Phys. Rev. Lett. **95**, 180401 (2005).